Aerodynamic Design Optimization for Natural Laminar Flow Airfoils

P. Paredes[1] P. Mysore[2] K. Jacobson[3] B. Diskin[4] N. Hildebrand[4] M. Choudhari[4]

[1]National Institute of Aerospace

[2]Georgia Institute of Technology

[3]Aeroelasticity Branch, NASA Langley Research Center

[4]Computational AeroSciences Branch, NASA Langley Research Center

AIAA Aviation 2024, AIAA Paper 2024-3529

CFD-01: Boundary Layer Transition Modeling and Applications I

9:30AM-9:50AM PDT, Room: Academy Ballroom 410. Las Vegas, NV. July 29, 2024

Outline

Natural Laminar Flow Technology

- Natural laminar flow (NLF) technology is a passive laminar flow control (LFC) strategy that seeks to delay the onset of boundary-layer transition (BLT) through shape optimization to reduce the viscous drag of the aerodynamic vehicle
- Viscous drag accounts for about 50% of the total drag of an aircraft[1]
- Laminar flow on wings at high Re can provide upto $\mathcal{O}(10\%)$ drag reduction on commercial aircrafts
- Drag reduction improves fuel efficiency that increases flight range and payload capacity, reduces operational costs, and lowers carbon emissions
- Boeing has recently included NLF technologies[2,3]:
  - 787-8 NLF Nacelles
  - 737Max NLF Winglet and Nacelles
  - 777X NLF Nacelles

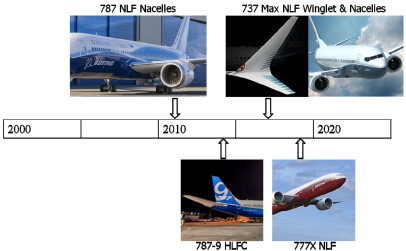

(Crouch 2015, AIAA Paper 2015-2472)

[1] R. Rashad and D.W. Zingg. *Viscous drag reduction on transport aircraft*. AIAA Paper 1991-0685. 1991.

[2] J.D. Crouch. *Broundary-layer transition prediction for laminar flow control*. AIAA Paper 2015-2472. 2015.

[3] M.R. Malik et al. "Application of Drag Reduction Techniques to Transport Aircraft". In: *Encyclopedia of Aerospace Engineering*. John Wiley & Sons, Ltd, 2015.

Natural Laminar Flow Design Optimization

- Optimization is critical to maximize the benefits of NLF technology
- Knowledge-based inverse-design optimization:
  - Crossflow Attenuated NLF (CATNLF)[4]
    - Successful design of transonic wind tunnel model, the CRM-NLF[5]
- Genetic algorithm design optimization:
  - Coupling of Euler solver with BL code and LST N-factor calculation[6]
- Physics-based adjoint design optimization:
  - Coupling of Euler solver with BL code and PSE N-factor calculation[7]
  - Coupling of RANS solver with BL code and N-factor surrogate[8,9,10]

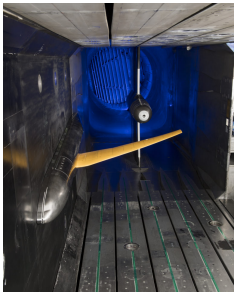

(https://commonresearchmodel.larc.nasa.gov/crm-nlf)

[4] R.L. Campbell and M.N. Lynde. *Natural laminar flow design for wings with moderate sweep*. AIAA Paper 2016-4326. 2016.

[5] M.N. Lynde and R.L. Campbell. *Computational design and analysis of a transonic natural laminar flow wing for a wind tunnel model*. AIAA Paper 2017-3058. 2017.

[6] D. Simanowitsch et al. *Comparison of Gradient-Based and Genetic Algorithms for Laminar Airfoil Shape Optimization*. AIAA Paper 2022-0008. 2022.

[7] O. Amoignon et al. "Shape Optimization for Delay of Laminar-Turbulent Transition". In: *AIAA Journal* 44.6 (2006), pp. 1009–1042.

[8] J.-D. Lee and A. Jameson. *Natural-Laminar-Flow Airfoil and Wing Design by Adjoint Method and Automatic Transition Prediction*. AIAA Paper 2009-0897. 2009.

[9] R. Rashad and D.W. Zingg. *Aerodynamic shape optimization for natural laminar flow using a discrete-adjoint approach*. AIAA Paper 2015-3061. 2015.

[10] Y. Shi et al. "Natural Laminar-Flow Airfoil Optimization Design Using a Discrete Adjoint Approach". In: *AIAA Journal* 58.11 (2020), pp. 4702–4722.

Objectives

- **Transition Modeling:** Integration of physics-based BLT modeling based on N-factor method into FUN3D/SFE calculations (similar to previous work with FUN3D/FV and LASTRAC[11])
  - Direct coupling of RANS transitional solutions with N-factor calculation (no BL code)
  - Transition location based on N-factor envelope calculation based on linear stability analysis (LSA)
- **Design Optimization:** Fully-coupled physics-based adjoint design optimization of BLT control strategies to target improvement of aerodynamic performance of the vehicle
  - Sensitivities to transition location incorporated through fully-coupled adjoint of CFD, mesh deformation, and transition prediction solvers

[11] N. Hildebrand et al. *Coupling of the FUN3D Unstructured Flow Solver and the LASTRAC Stability Code to Model Transition*. AIAA Paper 2022-1952. 2022.

Outline

NLF Design Optimization with Adjoint-Based Sensitivities

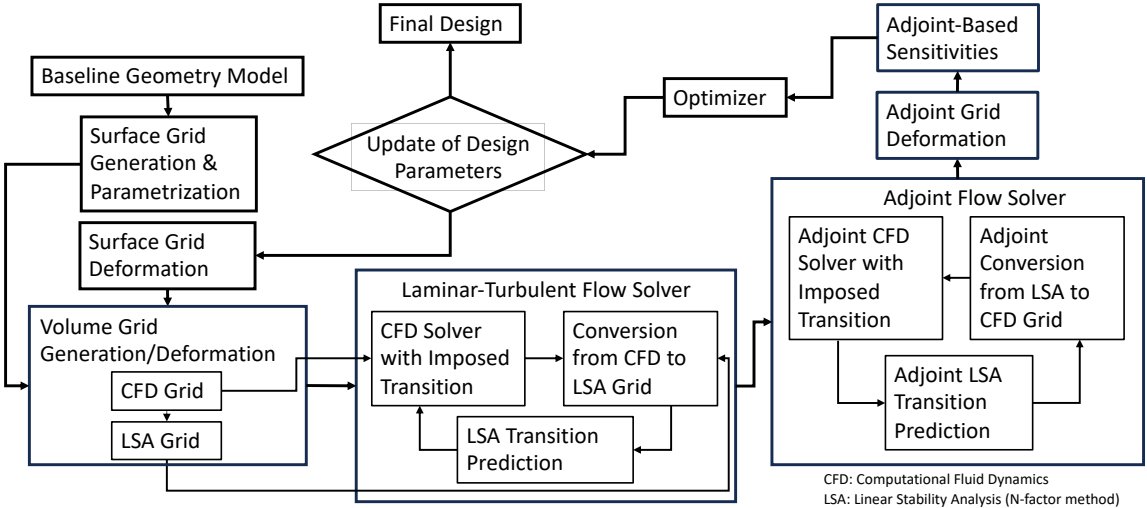

CFD: Computational Fluid Dynamics
LSA: Linear Stability Analysis (N-factor method)

Coupled Adjoint Formulation

- Adjoint problem formulated by defining the Lagrangian $\mathcal{L}$ based on the objective function $\mathbf{J}$ to be optimized
- Lagrangian contains $\mathbf{J}$ and set of residuals from the forward coupling
- Lagrangian multipliers $\boldsymbol{\lambda}$ are the adjoint variables

$$\begin{aligned}\mathcal{L}(\mathbf{d},\mathbf{x}_s,\mathbf{x},\boldsymbol{\xi},\xi_T,\gamma,\mathbf{Q},\bar{\mathbf{q}}) \;=\; & \mathbf{J}(\mathbf{x},\mathbf{Q},\mathbf{d}) + \boldsymbol{\lambda}_D^T \overbrace{\mathbf{D}(\mathbf{d},\mathbf{x}_s)}^{\text{shape deformation}} + \boldsymbol{\lambda}_G^T \overbrace{\mathbf{G}(\mathbf{x}_s,\mathbf{x})}^{\text{grid deformation}} + \boldsymbol{\lambda}_\xi^T \overbrace{\mathbf{K}_\xi(\mathbf{x}_s,\boldsymbol{\xi})}^{\text{LSA grid}} \\ & + \boldsymbol{\lambda}_\gamma^T \underbrace{\boldsymbol{\Gamma}(\boldsymbol{\xi},\xi_T,\gamma)}_{\text{intermittency}} + \boldsymbol{\lambda}_R^T \underbrace{\mathbf{R}(\mathbf{d},\mathbf{x},\gamma,\mathbf{Q})}_{\text{CFD flow solution}} + \boldsymbol{\lambda}_q^T \underbrace{\mathbf{K}_\mathbf{q}(\mathbf{x},\boldsymbol{\xi},\mathbf{Q},\bar{\mathbf{q}})}_{\text{LSA base flow}} + \boldsymbol{\lambda}_T^T \underbrace{\mathbf{T}(\boldsymbol{\xi},\bar{\mathbf{q}},\xi_T)}_{\text{transition location}}\end{aligned}$$

- Adjoint equations derived by differentiating $\mathcal{L}$ wrt design variables, $\mathbf{d}$, and collecting and setting to zero the coefficients of the derivatives wrt state variables, $\mathbf{x}_s,\mathbf{x},\boldsymbol{\xi},\xi_T,\gamma,\mathbf{Q},\bar{\mathbf{q}}$
- Adjoint-based sensitivities:

$$\frac{d\mathcal{L}}{d\mathbf{d}} = \frac{\partial \mathbf{J}}{\partial \mathbf{d}} + \boldsymbol{\lambda}_D^T \frac{\partial \mathbf{D}}{\partial \mathbf{d}} + \boldsymbol{\lambda}_R^T \frac{\partial \mathbf{R}}{\partial \mathbf{d}}$$

Surface and Volume Grid Deformation

- **Surface grid deformation:** Free-form deformation (FFD) method[12] used for surface parametrization and deformation
  - RAE 2822 airfoil with FFD box of 9x3 control points

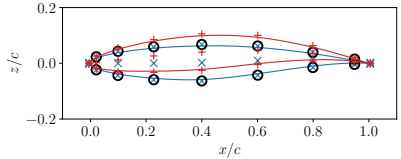

- **Volume grid deformation:** Linear elasticity model[13] used to displace volume nodes as a function of surface deformation
  - RAE 2822 airfoil

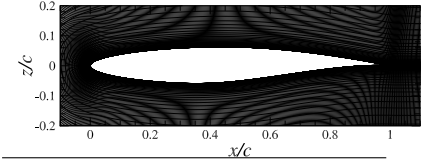

  - Deformed airfoil

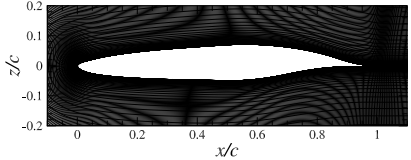

[12] T.W. Sederberg and S.R. Parry. "Free-Form Deformation of Solid Geometric Models". In: *SIGGRAPH Computer Graphics* 20 (1986), pp. 151–160.

[13] E.J. Nielsen and W.K. Anderson. "Recent improvements in aerodynamic design optimization on unstructured meshes". In: *AIAA Journal* 40.6 (2002), pp. 1155–1163.

Transition Prediction Coupled with FUN3D

- **CFD solver:** FUN3D/SFE solver[14] based on second-order finite-element discretization with negative version of Spalart-Allmaras RANS model
- **Transition prediction:** Dual N-factor based on LST of planar TS and stationary CF instabilities
- **Laminar-turbulence model:** Intermittency function γ is a multiplier of the turbulence production term[15,16]

$$\gamma(\xi, \xi_T) = \begin{cases} 1 - \exp\left[-0.413\left(\frac{3.36(\xi - \xi_T)}{l_T(\xi_T)}\right)^2\right], \; Re_{l_T} = 5.2 Re_{\xi_T}^{3/4} & \text{if} \quad \xi \geq \xi_T \\ 0 & \text{if} \quad \xi < \xi_T, \end{cases}$$

Iterative method to model transitional flow

1. Calculate mean flow solution with defined $\gamma(\xi_{T,i})$
2. Convert near wall laminar-flow solution from CFD to LSA grid
3. Perform LSA and define a new $\gamma(\xi_{T,i+1})$
4. Check convergence, i.e., $|\xi_{T,i+1} - \xi_{T,i}| < \epsilon_T$, and go to step 1 if not satisfied

[14] W.K. Anderson, J.C. Newman, and S.L. Karman. *Stabilized finite elements in FUN3D.* AIAA Paper 2017-0077. 2017.

[15] S. Dhawan and R. Narasimha. "Some Properties of Boundary Layer Flow During the Transition from Laminar to Turbulent Motion". In: *Journal of Fluid Mechanics* 3.4 (1958), pp. 418–436.

[16] G.J. Walker. "Transition Flow on Axial Turbomachine Blading". In: *AIAA Journal* 27.5 (1989), pp. 595–602.

The Dual *N*-factor Criterion[20]

- The logarithmic amplification ratio or *N*-factor is defined as

$$N(\xi, \omega, \beta) = -\int_{\xi_I}^{\xi} \sigma(\xi', \omega, \beta)\, \mathrm{d}\xi'$$

- $\sigma(\xi', \omega, \beta)$: Disturbance growth rate calculated with spatial LST eigenvalue analysis
- Transition onset predicted where the dual N-factor indicator function reaches 1, $I_N = N_d(N_{TS}, N_{CF}) = 1$

$$I_N = N_d(N_{TS}, N_{CF}) = \left(\frac{N_{TS}}{N_{TS,c}}\right)^{a_{TS}} + \left(\frac{N_{CF}}{N_{CF,c}}\right)^{a_{CF}}$$

- N_{CF}: *N*-factor envelope of stationary CF waves ($\omega = 0$)
- N_{TS}: *N*-factor envelope of TS waves approximated by the envelope of planar waves ($\beta = 0$) in a rotated orthogonal coordinate system aligned with $\mathbf{u}_\infty$
- Demonstrated and validated for a subsonic aircraft model[17] and the transonic CRM-NLF model[18]
- Discrete adjoint implementation of spatial LST eigenvalue analysis similar to previous work[19]

[17] A. Leidy et al. *Measurements and Computations of Natural Transition on the NASA Juncture-Flow Model with a Symmetric Wing*. AIAA Paper 2023-0441. 2023.

[18] P. Paredes et al. *Transition Modeling based on the Dual N-factor Method for the CRM-NLF Wind Tunnel Configuration*. AIAA Paper 2023-3532. 2023.

[19] C. Klauss et al. *Eigenvalue sensitivity computations for linear stability theory*. AIAA Paper 2023-3271. 2023.

[20] D. Arnal. "Boundary layer transition: Prediction based on linear theory". In: *Special course on Progress in Transition Modeling. AGARD. R-793*. 1994, pp. 1–62.

Outline

Flow Conditions and Optimization Parameters

- RAE 2822 airfoil used to evaluate coupled adjoint formulation for design optimization
  - Unswept, 2D BL case: $\Lambda = 0^\circ$, $C_{L,d} = 0.3$, symmetric spanwise BCs
  - Swept, 3D BL case: $\Lambda = 30^\circ$, $C_{L,d} = 0.225$, zero-order extrapolation spanwise BCs
- Optimizer: SNOPT, gradient-based optimizer with sequential quadratic programming method
- Objective function: $\mathbf{J} = C_D$
- Constraints: $C_L = C_{L,d}$, $A \leq A_0$ (area), $t_{cp} > 0.5 t_{cp,0}$ (thickness)
- Design variables: AoA, vertical displacement of 14 FFD control points (black circles)
- NASA FUN3D/SFE solver: NS solver for unstructured grids with finite-element discretization
- CGT[21]: c-type structured grid with $1,521 \times 2 \times 151$ points (721 in airfoil surface, 75 in BL at midchord)

- RAE 2822 airfoil with FFD box

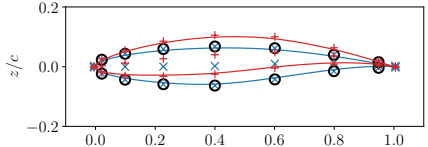

- Near-wall grid view

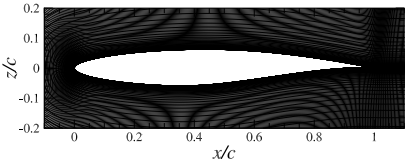

[21] W. Chan et al. *Best practices in overset grid generation.* AIAA Paper 2002-3191. 2002.

Computational Details and Verification of Adjoint-Based Sensitivities

- Dual N-factor parameters for transition modeling:
  - $N_{TS,c} = 9$, $N_{CF,c} = 7$, $a_{TS} = 1$, $a_{CF} = 2.5$
- Convergence thresholds:
  - RANS residual: $\epsilon_R = 10^{-13}$
  - Linear grid deformation: $\epsilon_G = 10^{-13}$
  - LST eigenvalue problem with Newton-Raphson iterations: $\epsilon_{LST} = 10^{-9}$
  - Transition location: $\epsilon_T = 10^{-8}$
- Adjoint implementation verified by comparing adjoint-based and real-step central FD sensitivities

	Adjoint	Central FD ($h = 10^{-6}$)
$d(C_D)/d(AoA)$	1.208×10^{-3}	1.207×10^{-3}
$d(C_L)/d(AoA)$	7.856×10^{-2}	7.862×10^{-2}
$d(C_D)/d(FFD_z)$	1.875×10^{-1}	1.887×10^{-1}
$d(C_L)/d(FFD_z)$	-1.391	-1.402

- Relative errors are $\mathcal{O}(10^{-3})$ with selected FD step size and convergence thresholds
- Similar relative errors found for a linearized frequency-domain gust analysis with FUN3D/SFE[22]

[22] K.E. Jacobson, A.S. Thelen, and B.K. Stanford. *Linearized Frequency-Domain Gust Analysis and Adjoint-Based Sensitivities*. AIAA Paper 2024-2591. 2024.

Computational Details and Verification of Adjoint-Based Sensitivities

- Dual N-factor parameters for transition modeling:
  - $N_{TS,c} = 9$, $N_{CF,c} = 7$, $a_{TS} = 1$, $a_{CF} = 2.5$
- Convergence thresholds:
  - RANS residual: $\epsilon_R = 10^{-13}$
  - Linear grid deformation: $\epsilon_G = 10^{-13}$
  - LST eigenvalue problem with Newton-Raphson iterations: $\epsilon_{LST} = 10^{-9}$
  - Transition location: $\epsilon_T = 10^{-8}$
- Adjoint implementation verified by comparing adjoint-based and real-step central FD sensitivities

	Adjoint	Central FD ($h = 10^{-6}$)
$d(C_D)/d(AoA)$	1.208×10^{-3}	1.207×10^{-3}
$d(C_L)/d(AoA)$	7.856×10^{-2}	7.862×10^{-2}
$d(C_D)/d(FFD_z)$	1.875×10^{-1}	1.887×10^{-1}
$d(C_L)/d(FFD_z)$	-1.391	-1.402

- Relative errors are $\mathcal{O}(10^{-3})$ with selected FD step size and convergence thresholds
- Similar relative errors found for a linearized frequency-domain gust analysis with FUN3D/SFE[22]
- For a fixed ξ_T, sensitivities become $d(C_D)/d(AoA) = 9.840 \times 10^{-5}$ and $d(C_D)/d(FFD_z) = -2.760 \times 10^{-4}$
  - Highlights importance of accounting for the effects of ξ_T variations

[22] K.E. Jacobson, A.S. Thelen, and B.K. Stanford. *Linearized Frequency-Domain Gust Analysis and Adjoint-Based Sensitivities*. AIAA Paper 2024-2591. 2024.

Unswept RAE 2822 Airfoil

- Flow conditions: $M_\infty = 0.19$, $Re_c = 5.6 \times 10^6$, $T^*_\infty = 300$ K, $\Lambda = 0°$, $AoA_0 = 0.72°$, $C_{L,d} = 0.3$
- 2D boundary layer: $N_{CF} = 0$, $N_d = N_{TS}/9$

- $C_D/C_{D,0}$, $C_L/C_{L,d}$, $x_T/x_{T,0}$

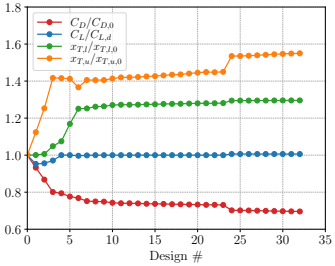

- Shape and C_p of #0 & #32

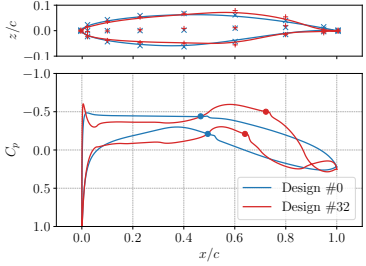

- N-factors of iteration #32

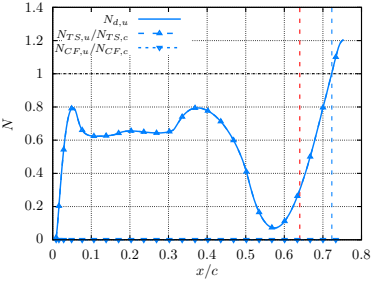

- Optimized airfoil #32: $AoA_{32} = 1.057°$, $C_{D,32}/C_{D,0} = 0.7$ (30% drag reduction)
- Additional design iterations required to reach optimum shape for NLF

Unswept RAE 2822 Airfoil

- Flow conditions: $M_\infty = 0.19$, $Re_c = 5.6 \times 10^6$, $T^*_\infty = 300$ K, $\Lambda = 0°$, $AoA_0 = 0.72°$, $C_{L,d} = 0.3$
- 2D boundary layer: $N_{CF} = 0$, $N_d = N_{TS}/9$

- $C_D/C_{D,0}$, $C_L/C_{L,d}$, $x_T/x_{T,0}$

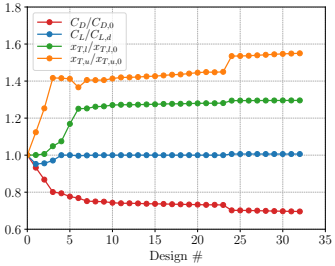

- Shape and C_p of #0 & #32

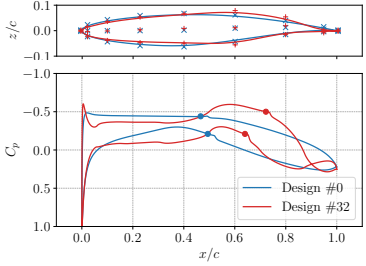

- N-factors of iteration #32

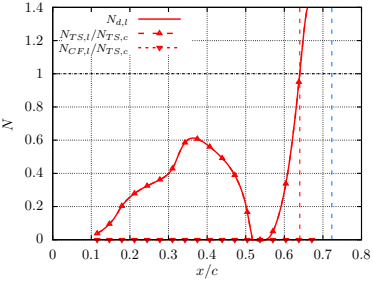

- Optimized airfoil #32: $AoA_{32} = 1.057°$, $C_{D,32}/C_{D,0} = 0.7$ (30% drag reduction)
- Additional design iterations required to reach optimum shape for NLF

Unswept RAE 2822 Airfoil

- Flow conditions: $M_\infty = 0.19$, $Re_c = 5.6 \times 10^6$, $T^*_\infty = 300$ K, $\Lambda = 0°$, $AoA_0 = 0.72°$, $C_{L,d} = 0.3$
- 2D boundary layer: $N_{CF} = 0$, $N_d = N_{TS}/9$

- $C_D/C_{D,0}$, $C_L/C_{L,d}$, $x_T/x_{T,0}$

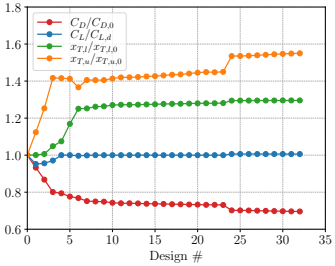

- Shape and C_p of #0 & #32

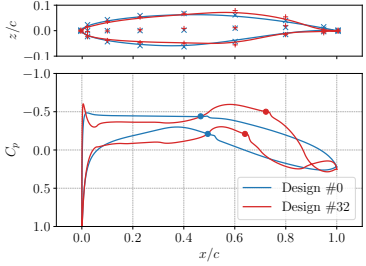

- N-factors of iteration #32

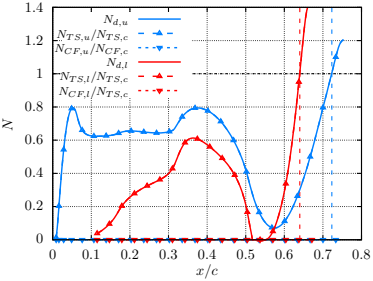

- Optimized airfoil #32: $AoA_{32} = 1.057°$, $C_{D,32}/C_{D,0} = 0.7$ (30% drag reduction)
- Additional design iterations required to reach optimum shape for NLF

Swept RAE 2822 Airfoil

- Flow conditions: $M_\infty = 0.19$, $Re_c = 5.6 \times 10^6$, $T^*_\infty = 300$ K, $\Lambda = 30°$, $AoA_0 = 0.72°$, $C_{L,d} = 0.225$
- 3D boundary layer: $N_d = (N_{TS}/9) + (N_{CF}/7)^{2.5}$ ($N_{CF} > 0$ only in lower side)
  - $C_D/C_{D,0}$, $C_D/C_{D,d}$, $x_T/x_{T,0}$
  - Shape and C_p of #0 & #4
  - N-factors of iteration #4

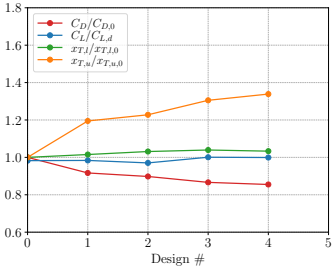

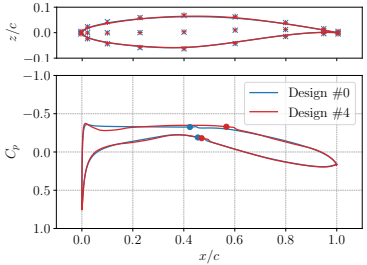

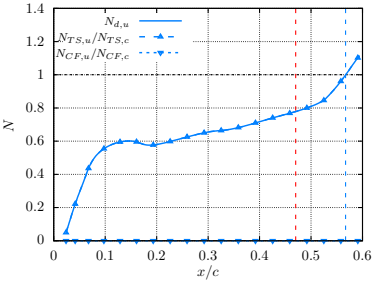

- Optimized airfoil (iteration #4): $AoA_4 = 0.658°$, $C_{D,4}/C_{D,0} = 0.855$ (14.5% drag reduction)
- Additional design iterations expected to further reduce drag

Swept RAE 2822 Airfoil

- Flow conditions: $M_\infty = 0.19$, $Re_c = 5.6 \times 10^6$, $T_\infty^* = 300$ K, $\Lambda = 30°$, $AoA_0 = 0.72°$, $C_{L,d} = 0.225$
- 3D boundary layer: $N_d = (N_{TS}/9) + (N_{CF}/7)^{2.5}$ ($N_{CF} > 0$ only in lower side)
  - $C_D/C_{D,0}$, $C_D/C_{D,d}$, $x_T/x_{T,0}$
  - Shape and C_p of #0 & #4
  - N-factors of iteration #4

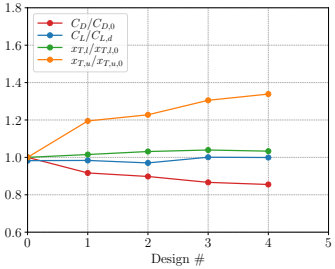

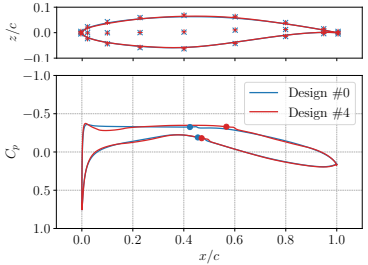

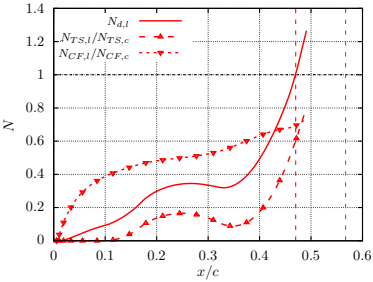

- Optimized airfoil (iteration #4): $AoA_4 = 0.658°$, $C_{D,4}/C_{D,0} = 0.855$ (14.5% drag reduction)
- Additional design iterations expected to further reduce drag

Swept RAE 2822 Airfoil

- Flow conditions: $M_\infty = 0.19$, $Re_c = 5.6 \times 10^6$, $T^*_\infty = 300$ K, $\Lambda = 30°$, $AoA_0 = 0.72°$, $C_{L,d} = 0.225$
- 3D boundary layer: $N_d = (N_{TS}/9) + (N_{CF}/7)^{2.5}$ ($N_{CF} > 0$ only in lower side)
  - $C_D/C_{D,0}$, $C_D/C_{D,d}$, $x_T/x_{T,0}$

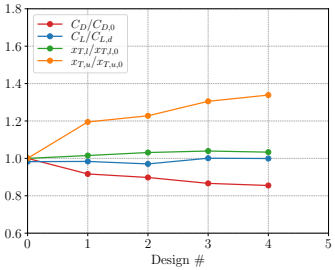

  - Shape and C_p of #0 & #4

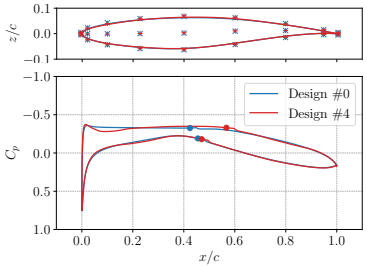

  - N-factors of iteration #4

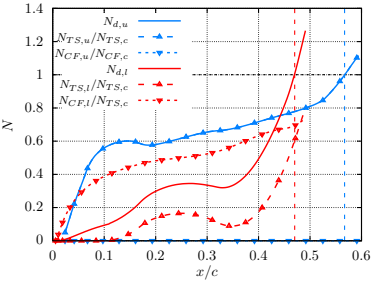

- Optimized airfoil (iteration #4): $AoA_4 = 0.658°$, $C_{D,4}/C_{D,0} = 0.855$ (14.5% drag reduction)
- Additional design iterations expected to further reduce drag

Outline

Summary and Concluding Remarks

- Implementation of physics-based aerodynamic design optimization of unswept and swept airfoils for natural laminar flow
  - Adjoint-based design optimization formulation with NASA FUN3D/SFE, linear grid deformation, and physics-based transition modeling based on linear stability analysis
  - Iterative transition modeling method with NASA FUN3D/SFE based on dual N-factor criterion with LST spatial eigenvalue problem that accounts for linear amplification of planar TS and stationary CF waves
- Preliminary optimization results with unswept and swept airfoils at subsonic conditions achieve significant drag reductions by shifting transition locations downstream over both airfoil sides
- Future work:
  - Perform additional design iterations to reach optimal airfoil shapes
  - Extend the analysis to transonic and supersonic conditions
  - Apply the optimization to 3D NLF wing design

Thank you for your attention

- Acknowledgements
  - This material is based upon work supported by
    - the NASA Transformational Tools and Technologies (TTT) Project of the Transformative Aeronautics Concepts Program (TACP) under the Aeronautics Research Mission Directorate (ARMD)
    - the Air Force Office of Scientific Research under award number FA9550-20-0023
  - Computational Resources supporting this work are provided by
    - Department of Defense (DOD) High Performance Computing Modernization Program (HPCMP)
    - NASA High-End Computing (HEC) Program through the NASA Advanced Supercomputing (NAS) Division at Ames Research Center
    - NASA K cluster at the Langley Research Center